AIAA JOURNAL
Vol. 47, No. 7, July 2009

Asymptotic Solution for Nonlinear Buckling of Orthotropic Shells on Elastic Foundation

G. H. Nie*
Tongji University, 200092 Shanghai, People's Republic of China
C. K. Chan†
Hong Kong Polytechnic University, Hung Hom, Kowloon, Hong Kong, People's Republic of China
J. C. Yao‡
Tongji University, 200092 Shanghai, People's Republic of China
and
X. Q. He§
City University of Hong Kong, Kowloon Tong, Hong Kong, People's Republic of China

DOI: 10.2514/1.43311

An asymptotic solution for nonlinear buckling of elastically restrained imperfect, orthotropic, shallow spherical shells on an elastic foundation is derived in this paper. An analytic and explicit relation between external pressure and central deflection of the shell is presented in nondimensional form using the asymptotic iteration method. The solution incorporates the effects of orthotropic and material parameters, geometric imperfection, Young's and shear moduli of foundation, and edge-restraint coefficients. An extensive parametric study is carried out for deformation and buckling of such structures. Comparisons with available data for some specific cases show that the resulting solution is accurate in computation. It also indicates that the present solution can be readily used to evaluate nonlinear deformation and buckling behavior of orthotropic, imperfect, shallow spherical shells.

Nomenclature

$D = \frac{E_\theta h^3}{12(\beta - \nu_\theta^2)}$	=	flexural rigidity
E_r, ν_r	=	elastic modulus and Poisson's ratio in the radial direction
E_θ, ν_θ	=	elastic modulus and Poisson's ratio in the circumferential direction
G	=	nondimensional shear modulus of foundation
g	=	shear modulus of foundation
H	=	apex height of the shell
h	=	thickness of the shell
K_b, K_i	=	nondimensional rotational and in-plane edge-restraint coefficients
K_1, K_3	=	nondimensional Young's moduli of foundation
k_1, k_3	=	Young's moduli of foundation
$P = \frac{qa^4}{E_\theta h^4}$	=	nondimensional uniformly distributed load
q	=	uniformly distributed normal load
q_0	=	external pressure due to elastic foundation
R	=	radius of curvature of the shell
u	=	radial displacement
W	=	nondimensional transverse displacement (deflection)
w	=	transverse displacement (deflection)
W_m	=	nondimensional central transverse displacement (deflection)
W_0	=	imperfection factor
W^i	=	nondimensional geometric imperfection
w^i	=	geometric imperfection
$\beta = \frac{E_\theta}{E_r} = \frac{\nu_\theta}{\nu_r}$	=	orthotropic parameter
$\lambda = \frac{a^2}{Rh} \approx \frac{2H}{h}$	=	characteristic geometric parameter
ξ, η	=	rotational and in-plane edge-restraint coefficients
$\Phi = \frac{a\phi}{D}$	=	nondimensional force function
ϕ	=	force function
$2a$	=	span of the shell

Received 30 January 2009; revision received 5 April 2009; accepted for publication 6 April 2009.

*Professor, Institute of Applied Mechanics, School of Aerospace Engineering and Applied Mechanics.
†Professor, Department of Applied Mathematics. Senior Member AIAA.
‡Graduate Student, Institute of Applied Mechanics, School of Aerospace Engineering and Applied Mechanics.
§Lecturer, Department of Building and Construction.

I. Introduction

The thin spherical shell, as an important structural component, has extensive applications in many engineering fields. Deformation of such structures under an external load causes the phenomenon of snap-through buckling. Evaluation of such buckling behavior and critical load becomes an important topic in research. A lot of work on buckling analysis has been carried out for perfect shallow spherical shell structures [1–12]. As flexible structures, shallow spherical shells are sensitive to initial geometric imperfections. The effect of imperfection on load carrying capability is thus important in buckling analysis of such imperfect structures [13–17]. In addition, the effects of the elastic foundation supporting the shells on deformation and buckling behaviors of the structures are also important. The structure–foundation interactions are frequently considered using linear and nonlinear Winkler and Pasternak foundations [18–28].

The fundamental governing equations of equilibrium and compatibility for shallow shell structures are coupled, and an exact solution for nonlinear problems does not exist. Accordingly, many approximate methods have been developed to solve the corresponding problems, such as methods containing a Bessel and Chebyshev series, Galerkin's method, Berger's method, a modified Berger's method, Sinharay and Banerjee's method, a finite difference method, and a finite element method. Galerkin or various weighted residual methods are frequently used among these methods. With different boundary conditions, corresponding trial functions of spatial distribution for displacements can be presumed, and approximate expressions for mechanical behavior can be obtained. Although such treatment has proved to be effective, the procedure causes errors because the governing equations are not solved exactly. On the other hand, existing studies focus mostly on

simple boundary conditions such as movable or immovable simply supported and clamped edges. However, in practice they are generally elastically restrained against rotation and nonuniformly supported along its edge or edges [7,27,28]. Hence, an analytic solution is of great importance for the understanding of deformation and buckling behavior of imperfect shallow spherical shells with an elastically restrained edge resting on an elastic foundation. In seeking for an analytic formulation of nonlinear static and dynamic behavior of shallow shell structures, an asymptotic iteration method (AIM) is proposed and applied to nonlinear buckling and vibration of imperfect and perfect reticulated (latticed) shallow spherical shells and solid shallow spherical shells on elastic foundations [27–31]. AIM is similar to the perturbation technique in that the solution is initially constructed based on the use of a linear solution for transverse displacement (deflection). However, the two techniques are different in that during the process of each iteration of the AIM, the same equation for the central deflection is introduced in the derivation of both load-central deflection and force function-central deflection relations, whereas the load remains unchanged for each iteration. AIM results in more terms than the perturbation, which is based on series expansion of deflection, force function, and the load in terms of the central deflection, respectively, if chosen as perturbation parameters. AIM is therefore a modified successive iterative method but generally with improved speed of convergence. For membrane force, it is determined by solving the exact compatibility equation instead of a linearized equation as commonly done in perturbation methods. By means of central deflection as a perturbation parameter in the process of iteration, an analytic expression between the load and central deflection is finally derived.

There have been relatively few studies on the buckling of orthotropic perfect and imperfect shallow spherical shells [6,7,16,19,25,26]. In this paper, an asymptotic solution is developed for nonlinear behavior of orthotropic, shallow spherical shells with imperfections resting on an elastic foundation under uniform external pressure. The shell is elastically restrained against rotational, transverse, and in-plane displacements. Geometric imperfection is assumed to have the same mode as that of transverse displacement, but no specific form of the mode is presumed. An analytic and explicit relation in nondimensional form between pressure and central deflection of the shell is derived based on the AIM. Numerical examples are given to illustrate the validity of the resulting solution and effects of geometric and material parameters, imperfection, moduli of foundation, and edge restraint on deformation and buckling of such structures.

II. Mathematical Formulation

Consider an imperfect shallow spherical shell subjected to uniform normal pressure q on a convex surface and supported on an elastic foundation, as shown in Fig. 1. It is assumed that the foundation is made up of massless springs with shear interaction among them. The foundation is characterized by extensional and shear moduli k_1, k_3, and g respectively.

The relation between internal force and strains (displacements) can be written as

$$\varepsilon_r = \frac{1}{Eh}(\beta N_r - \nu N_\theta), \qquad \varepsilon_\theta = \frac{1}{Eh}(N_\theta - \nu N_r) \tag{1}$$

$$M_r = -D\left(\frac{\mathrm{d}^2 w}{\mathrm{d}r^2} + \frac{\nu}{r}\frac{\mathrm{d}w}{\mathrm{d}r}\right), \qquad M_\theta = -D\left(\frac{\beta}{r}\frac{\mathrm{d}w}{\mathrm{d}r} + \nu\frac{\mathrm{d}^2 w}{\mathrm{d}r^2}\right) \tag{2}$$

denoting $E = E_\theta$ and $\nu = \nu_\theta$. Assuming that there is an initial geometric imperfection w^i, the geometric equations are given by

$$\varepsilon_r = \frac{\mathrm{d}u}{\mathrm{d}r} - \frac{w}{R} + \frac{1}{2}\left(\frac{\mathrm{d}w}{\mathrm{d}r}\right)^2 + \frac{\mathrm{d}w}{\mathrm{d}r}\frac{\mathrm{d}w^i}{\mathrm{d}r} \tag{3}$$

$$\varepsilon_\theta = \frac{u}{r} - \frac{w}{R} \tag{4}$$

and the equilibrium equations for in-plane internal forces and moments are given by

$$\frac{\mathrm{d}}{\mathrm{d}r}(rN_r) - N_\theta = 0 \tag{5}$$

$$\frac{\mathrm{d}}{\mathrm{d}r}(rM_r) - M_\theta - rQ_r = 0 \tag{6}$$

With the effect of external pressure q_0 due to elastic foundation, or $q_0 = k_1 w + k_3 w^3 - g\nabla^2 w$, the equilibrium equation in the normal direction can be expressed as

$$\frac{\mathrm{d}}{\mathrm{d}r}\left\{rN_r\left[\frac{r}{R} + \frac{\mathrm{d}(w + w_i)}{\mathrm{d}r}\right] + rQ_r\right\} + r(q - q_0) = 0 \tag{7}$$

Introducing a force function ϕ defined by

$$N_r = \frac{\phi}{r} \quad \text{and} \quad N_\theta = \frac{\mathrm{d}\phi}{\mathrm{d}r} \tag{8}$$

Eq. (5) is satisfied automatically. Applying Eqs. (2), (6), and (8), Eq. (7) can be expressed in terms of w and ϕ such that

$$D\frac{1}{r}\frac{\mathrm{d}}{\mathrm{d}r}\left(r\frac{\mathrm{d}^3 w}{\mathrm{d}r^3} + \frac{\mathrm{d}^2 w}{\mathrm{d}r^2} - \frac{\beta}{r}\frac{\mathrm{d}w}{\mathrm{d}r}\right) = \frac{1}{r}\frac{\mathrm{d}}{\mathrm{d}r}\left\{\phi\left[\frac{r}{R} + \frac{\mathrm{d}(w + w_i)}{\mathrm{d}r}\right]\right\} - k_1 w - k_3 w^3 + g\nabla^2 w + q \tag{9}$$

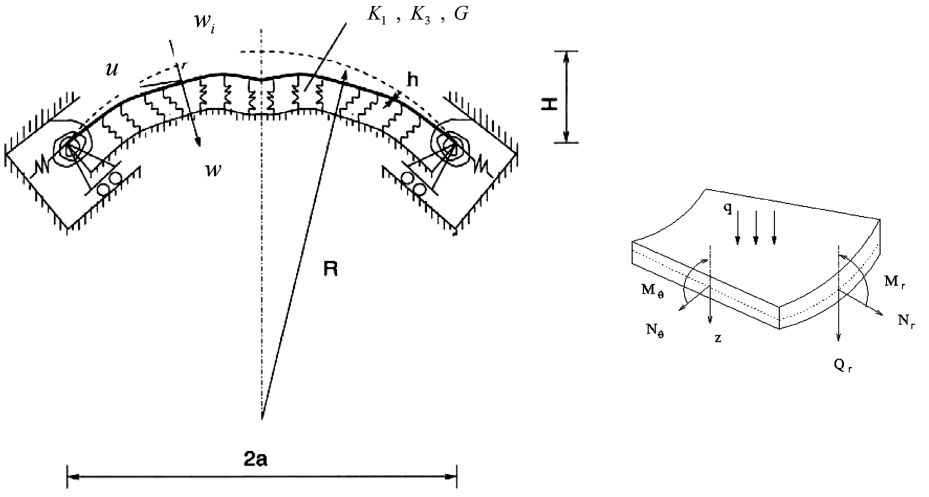

Fig. 1 Geometry and internal forces of an imperfect, orthotropic, shallow spherical shell.

On the other hand, using Eqs. (1) and (8), the compatibility equation can be obtained by eliminating the radial displacement u in geometric Eqs. (3) and (4) as

$$r\frac{\mathrm{d}^2\phi}{\mathrm{d}r^2}+\frac{\mathrm{d}\phi}{\mathrm{d}r}-\frac{\beta}{r}\phi=-Eh\frac{\mathrm{d}w}{\mathrm{d}r}\left[\frac{r}{R}+\frac{1}{2}\frac{\mathrm{d}(w+w_i)}{\mathrm{d}r}\right] \tag{10}$$

Consider an elastically restrained boundary against rotational, transverse, and in-plane displacements [27]

$$w=0,\qquad M_r=\xi\frac{\mathrm{d}w}{\mathrm{d}r},\qquad N_r=-\eta u\quad \text{at } r=a \tag{11}$$

where ξ and η are the rotational and in-plane edge-constraint coefficients, respectively. At the center of the shell

$$w<\infty,\qquad \frac{\mathrm{d}w}{\mathrm{d}r}=0,\qquad rN_r=0\quad \text{at } r=0 \tag{12}$$

Introducing the nondimensional quantities

$$\begin{aligned}&\rho=\frac{r}{a},\quad W=\frac{w}{h},\quad W^i=\frac{w^i}{h},\quad \lambda_0=\frac{w^i}{w}=\frac{W^i}{W}=\frac{W_0}{W_m}\\&\lambda=\frac{a^2}{Rh}\approx\frac{2H}{h},\quad K_b=\frac{\xi a}{D},\quad K_i=\frac{\eta a}{Eh},\quad K_1=\frac{k_1a^4}{D}\\&K_3=\frac{k_3a^4h^2}{D},\quad G=\frac{ga^2}{D},\quad P=\frac{qa^4}{Eh^4},\quad \Phi=\frac{a}{D}\phi\end{aligned} \tag{13}$$

where $W_m=W|_{\rho=0}$ is nondimensional central transverse displacement (deflection) and $W_0=W^i|_{\rho=0}=w^i|_{r=0}/h$ is imperfection factor, and suppose that initial geometric imperfection has the same mode as that of transverse displacement (deflection), the von Kármán-type fundamental governing Eqs. (9) and (10) with boundary conditions (11) and (12) are written as

$$\begin{aligned}\rho^2\frac{\mathrm{d}^3W}{\mathrm{d}\rho^3}+\rho\frac{\mathrm{d}^2W}{\mathrm{d}\rho^2}-p^2\frac{\mathrm{d}W}{\mathrm{d}\rho}=\rho\Phi\left[\lambda\rho+(1+\lambda_0)\frac{\mathrm{d}W}{\mathrm{d}\rho}\right]\}+\frac{1}{2}eP\rho^3\\-K_1\rho\int_0^\rho W(\rho)\rho\mathrm{d}\rho-K_3\rho\int_0^\rho W^3(\rho)\rho\mathrm{d}\rho+G\rho^2\frac{\mathrm{d}W}{\mathrm{d}\rho}\end{aligned} \tag{14}$$

$$\rho^2\frac{\mathrm{d}^2\Phi}{\mathrm{d}\rho^2}+\rho\frac{\mathrm{d}\Phi}{\mathrm{d}\rho}-p^2\Phi=-e\rho\frac{\mathrm{d}W}{\mathrm{d}\rho}\left[\lambda\rho+\frac{1}{2}(1+2\lambda_0)\frac{\mathrm{d}W}{\mathrm{d}\rho}\right] \tag{15}$$

and

$$W=0,\qquad \frac{\mathrm{d}^2W}{\mathrm{d}\rho^2}+B_b\frac{1}{\rho}\frac{\mathrm{d}W}{\mathrm{d}\rho}=0,\qquad \frac{\mathrm{d}\Phi}{\mathrm{d}\rho}-B_i\frac{\Phi}{\rho}=0\quad \text{at } \rho=1 \tag{16}$$

$$\frac{\mathrm{d}W}{\mathrm{d}\rho}=0,\qquad \Phi=0\quad \text{at } \rho=0 \tag{17}$$

with

$$p=\beta^{1/2},\quad B_b=K_b+v,\quad B_i=-\frac{1}{K_i}+v,\quad e=12(\beta-\nu^2) \tag{18}$$

III. Asymptotic Iterations

A. First Approximation

Consider the reduced linear boundary-value problem formulated from the original governing equations in Eqs. (14–17) as

$$\rho^2\frac{\mathrm{d}^2V^{(1)}}{\mathrm{d}\rho^2}+\rho\frac{\mathrm{d}V^{(1)}}{\mathrm{d}\rho}-p^2V^{(1)}=\frac{1}{2}eP^{(1)}\rho^3 \tag{19}$$

$$\rho^2\frac{\mathrm{d}^2\Phi^{(1)}}{\mathrm{d}\rho^2}+\rho\frac{\mathrm{d}\Phi^{(1)}}{\mathrm{d}\rho}-p^2\Phi^{(1)}=-e\rho V^{(1)}\left[\lambda\rho+\frac{1}{2}(1+2\lambda_0)V^{(1)}\right] \tag{20}$$

and

$$\begin{aligned}&W^{(1)}=0,\qquad \frac{\mathrm{d}V^{(1)}}{\mathrm{d}\rho}+B_bV^{(1)}=0\\&\frac{\mathrm{d}\Phi^{(1)}}{\mathrm{d}\rho}-B_i\Phi^{(1)}=0\quad \text{at } \rho=1\end{aligned} \tag{21}$$

$$V^{(1)}=0,\qquad \Phi^{(1)}=0\quad \text{at } \rho=0 \tag{22}$$

where $V^{(1)}=\frac{\mathrm{d}W^{(1)}}{\mathrm{d}\rho}$. The superscript (1) represents the first approximated solution. Using the first two equations in Eq. (21) and the first equation in Eq. (22) to solve Eq. (19) yields the expressions for $W^{(1)}$ as

$$W^{(1)}=\frac{1}{a_3}(1+a_1\rho^{1+p}+a_2\rho^4)P^{(1)} \tag{23}$$

where

$$\begin{aligned}&a_1=\frac{4(B_b+3)}{(p-3)(p+B_b+4)},\qquad a_2=-\frac{(1+p)(p+B_b)}{(p-3)(p+B_b+4)}\\&a_3=\frac{8(1+p)(3+p)(B_b+p)}{e(p+B_b+4)}\end{aligned} \tag{24}$$

Denoting the nondimensional central deflection by

$$W^{(1)}(0)=W_m \tag{25}$$

the linear nondimensional relation between the load and the central deflection is obtained from Eq. (23) as

$$P^{(1)}=a_3W_m \tag{26}$$

Accordingly, $W^{(1)}$ can be expressed by W_m as

$$W^{(1)}=(1+a_1\rho^{1+p}+a_2\rho^4)W_m \tag{27}$$

Substituting Eq. (27) into Eq. (20) and using the third equation in Eq. (21) and the second one in Eq. (22), the solution for $\Phi^{(1)}(\rho)$ can be derived as

$$\Phi^{(1)}=f_1(\rho)W_m+f_2(\rho)W_m^2 \tag{28}$$

where

$$\begin{aligned}&f_1(\rho)=b_{10}\rho^p+b_{11}\rho^{2+p}+b_{12}\rho^{1+2p}+b_{13}\rho^{4+p}+b_{14}\rho^5+b_{15}\rho^7\\&f_2(\rho)=b_{20}\rho^p+b_{21}\rho^{1+2p}+b_{22}\rho^{4+p}+b_{23}\rho^7\end{aligned} \tag{29}$$

where coefficients $b_{ij}(i=1,2;j=0,1,2,\ldots,5)$ are shown in Appendix A. In view of Eq. (24), the preceding solutions for $W^{(1)}$, $V^{(1)}$, and $\Phi^{(1)}(\rho)$ are valid for $p\neq 3$. For $p=3$, the corresponding solution is presented in Sec. III.C.

B. Second Approximation

Consider the boundary-value problem

$$\begin{aligned}\rho^2\frac{\mathrm{d}^2V^{(2)}}{\mathrm{d}\rho^2}+\rho\frac{\mathrm{d}V^{(2)}}{\mathrm{d}\rho}-p^2V^{(2)}=\Phi^{(1)}\rho[\lambda\rho+(1+\lambda_0)V^{(1)}]\\-K_1\rho\int_0^\rho W^{(1)}\rho\mathrm{d}\rho-K_3\rho\int_0^\rho(W^{(1)})^3\rho\mathrm{d}\rho+G\rho^2V^{(1)}\\+\frac{1}{2}eP^{(2)}\rho^3\end{aligned} \tag{30}$$

and

$$W^{(2)}=0,\qquad \frac{\mathrm{d}V^{(2)}}{\mathrm{d}\rho}+B_bV^{(2)}=0\quad \text{at } \rho=1 \tag{31}$$

$$V^{(2)}=0\quad \text{at } \rho=0 \tag{32}$$

where $P^{(2)}$, $W^{(2)}$, and $V^{(2)}=\frac{\mathrm{d}W^{(2)}}{\mathrm{d}\rho}$ correspond to the second iteration solutions for P, W, and V, respectively. By means of expressions for

$W^{(1)}$, $V^{(1)}$, and $\Phi^{(1)}$ in Sec. III.A as reference variables, expressions for $W^{(2)}$ and $V^{(2)}$ may be obtained by solving Eq. (30). Noting that $W^{(2)}(0) = W_m$, there will be a characteristic relation between the load and the deflection at the center in a nondimensional form such that

$$P^{(2)} = \alpha_1 W_m + \alpha_2 W_m^2 + \alpha_3 W_m^3 \tag{33}$$

where

$$\alpha_1 = -\frac{8}{e}(9-p^2)\left(1+\sum_{i=0}^{13} c_{1i}\right), \qquad \alpha_2 = -\frac{8}{e}(9-p^2)\sum_{i=0}^{11} c_{2i}$$
$$\alpha_3 = -\frac{8}{e}(9-p^2)\sum_{i=0}^{12} c_{3i} \tag{34}$$

where coefficients $c_{si}(s = 1, 2, 3; i = 0, 1, 2, \ldots, 13)$ are expressed in Appendix A.

C. Solution for $p = 3$

When $p = 3$, the governing Eqs. (19) and (20) become

$$\rho^2\frac{\mathrm{d}^2V^{(1)}}{\mathrm{d}\rho^2} + \rho\frac{\mathrm{d}V^{(1)}}{\mathrm{d}\rho} - 9V^{(1)} = \frac{1}{2}eP^{(1)}\rho^3 \tag{35}$$

$$\rho^2\frac{\mathrm{d}^2\Phi^{(1)}}{\mathrm{d}\rho^2} + \rho\frac{\mathrm{d}\Phi^{(1)}}{\mathrm{d}\rho} - 9\Phi^{(1)} = -e\rho V^{(1)}\left[\lambda\rho + \frac{1}{2}(1+2\lambda_0)V^{(1)}\right] \tag{36}$$

and corresponding boundary conditions remain unchanged, as expressed in Eqs. (21) and (22). Following the same procedure as in Sec. III.A, the first iterated solution for Eq. (35) has the form

$$W^{(1)} = \left[1 + \left(a_4 - \frac{a_5}{4}\right)\rho^4 + a_5\rho^4\,\ell_n\,\rho\right]W_m \tag{37}$$

and the relation between the load and central deflection is thus

$$P^{(1)} = a_6 W_m \tag{38}$$

where

$$a_4 = -\frac{1}{4B_b+13}, \quad a_5 = \frac{B_b+3}{4B_b+13}, \quad a_6 = \frac{48(B_b+3)}{e(4B_b+13)} \tag{39}$$

The expression for $\Phi^{(1)}(\rho)$ has a form

$$\Phi^{(1)} = g_1(\rho)W_m + g_2(\rho)W_m^2 \tag{40}$$

where

$$g_1(\rho) = b_{10}\rho^3 + \rho^5(b_{11} + b_{12}\,\ell_n\,\rho) + \rho^7(b_{13} + b_{14}\,\ell_n\,\rho + b_{15}\ln^2\rho)$$
$$g_2(\rho) = b_{20}\rho^3 + \rho^7(b_{21} + b_{22}\,\ell_n\,\rho + b_{23}\ln^2\rho) \tag{41}$$

and the coefficients $b_{ij}(i = 1, 2; j = 0, 1, 2, \ldots, 5)$ are shown in Appendix B.

Further, consider the corresponding equation for $V^{(2)}$ and $W^{(2)}$

$$\rho^2\frac{\mathrm{d}^2V^{(2)}}{\mathrm{d}\rho^2} + \rho\frac{dV^{(2)}}{d\rho} - 9V^{(2)} = \Phi^{(1)}\rho[\lambda\rho + (1+\lambda_0)V^{(1)}] - K_1\rho\int_0^\rho W^{(1)}\rho\mathrm{d}\rho - K_3\rho\int_0^\rho (W^{(1)})^3\rho\mathrm{d}\rho + G\rho^2V^{(1)} + \frac{1}{2}eP^{(2)}\rho^3 \tag{42}$$

under conditions Eqs. (31) and (32), the final result corresponding to Eq. (33) is

$$P^{(2)} = \beta_1 W_m + \beta_2 W_m^2 + \beta_3 W_m^3 \tag{43}$$

where

$$\beta_1 = \frac{192}{e}\left(1 + c_{10} + \frac{c_{11}}{4} - \frac{c_{12}}{6} + \frac{c_{13}}{6} - \frac{c_{14}}{36} + \frac{c_{15}}{8} - \frac{c_{16}}{64} + \frac{c_{17}}{10} - \frac{c_{18}}{100} + \frac{c_{19}}{500} + \frac{c_{110}}{12} - \frac{c_{111}}{144} + \frac{c_{112}}{864} - \frac{c_{113}}{3456}\right)$$
$$\beta_2 = \frac{192}{e}\left(c_{20} + \frac{c_{21}}{6} + \frac{c_{22}}{8} - \frac{c_{23}}{64} + \frac{c_{24}}{10} - \frac{c_{25}}{100} + \frac{c_{26}}{500} + \frac{c_{27}}{12} - \frac{c_{28}}{144} + \frac{c_{29}}{864} - \frac{c_{210}}{3456}\right)$$
$$\beta_3 = \frac{192}{e}\left(c_{30} + \frac{c_{31}}{4} - \frac{c_{32}}{16} + \frac{c_{33}}{8} - \frac{c_{34}}{64} + \frac{c_{35}}{12} - \frac{c_{36}}{144} + \frac{c_{37}}{864} - \frac{c_{38}}{3456} + \frac{c_{39}}{16} - \frac{c_{310}}{256} + \frac{c_{311}}{2048} - \frac{c_{312}}{32768}\right) \tag{44}$$

and the coefficients $c_{si}(s = 1, 2, 3; i = 0, 1, 2, \ldots, 13)$ are shown in Appendix B.

To obtain the third approximation, the resulting expressions for $W^{(1),(2)}$, $V^{(1),(2)}$, and $\Phi^{(1)}$ are used as reference variables, and the corresponding boundary-value problem can be formulated as

$$\rho^2\frac{\mathrm{d}^2V^{(3)}}{\mathrm{d}\rho^2} + \rho\frac{\mathrm{d}V^{(3)}}{\mathrm{d}\rho} - p^2V^{(3)} = \lambda\rho^2\Phi^{(2)} + (1+\lambda_0)[\Phi^{(1)}V^{(2)} + \Phi^{(2)}V^{(1)}]\rho - K_1\rho\int_0^\rho W^{(2)}(\rho)\rho\mathrm{d}\rho - K_3\rho\int_0^\rho W^{(2)3}(\rho)\rho\mathrm{d}\rho + G\rho^2V^{(2)} + \frac{1}{2}eP^{(3)}\rho^3 \tag{45}$$

and

$$W^{(3)} = 0, \qquad \frac{\mathrm{d}V^{(3)}}{\mathrm{d}\rho} + B_bV^{(3)} = 0, \quad \text{at } \rho = 1 \tag{46}$$

$$W^{(3)}(0) = W_m, \qquad V^{(3)} = 0, \quad \text{at } \rho = 0 \tag{47}$$

where $\Phi^{(2)}$ can be determined by solving the following equation:

$$\rho^2\frac{\mathrm{d}^2\Phi^{(2)}}{\mathrm{d}\rho^2} + \rho\frac{\mathrm{d}\Phi^{(2)}}{\mathrm{d}\rho} - p^2\Phi^{(2)} = -e\rho V^{(2)}\left[\lambda\rho + (1+2\lambda_0)V^{(1)}\right] \tag{48}$$

with

$$\frac{\mathrm{d}\Phi^{(2)}}{\mathrm{d}\rho} - B_i\Phi^{(2)} = 0 \quad \text{at } \rho = 1 \tag{49}$$

$$\Phi^{(2)} = 0 \quad \text{at } \rho = 0 \tag{50}$$

where $Q^{(3)}$, $W^{(3)}$, and $V^{(3)} = \frac{\mathrm{d}W^{(3)}}{\mathrm{d}\rho}$ stand for the approximations for Q, W, and V respectively. Further iterative approximations can also be performed successively based on the preceding procedure depending on the required accuracy.

IV. Results

To validate the resulting solutions in Sec. III, comparisons of numerical results are initially made. For different foundation moduli K_1, K_3, and G, rotational and in-plane edge-restraint coefficients K_b and K_i, orthotropic parameter β, Poisson's ratio $\nu = \nu_\theta$, and the ratio of apex height H to the thickness of the shell h, changes in critical buckling loads $P_{\mathrm{cr}}^{(2)}$ and $P_{\mathrm{cr}}^{(3)}$ corresponding to the second and third approximations, respectively, determined with $\frac{\mathrm{d}P}{\mathrm{d}W_m} = 0$ for the resulting characteristic relations, are illustrated in Figs. 2–4, respectively. Results show that the values of buckling loads for the second and third approximations are very close, indicating the validity of the second approximation, which is similar in commonly used perturbation methods.

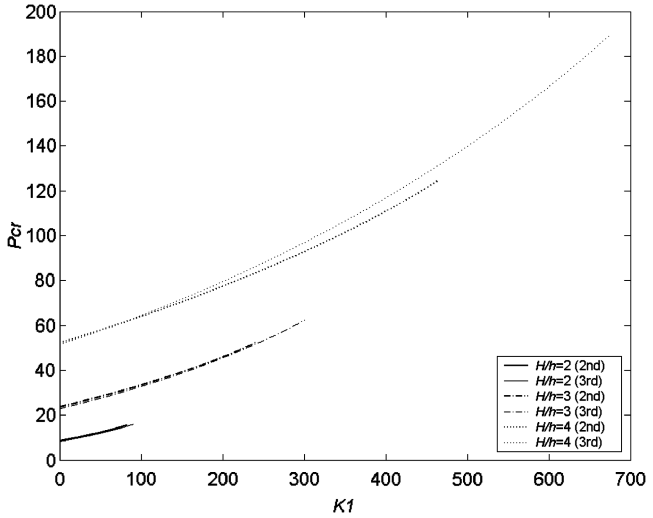

Fig. 2 Distribution of buckling load with foundation modulus ($\beta = 1$, $K_b = 2.0$, $K_i = 2.0$, $\nu = 0.3$, $H/h = 3$, $W_0 = 0$, $K_3 = G = 0$).

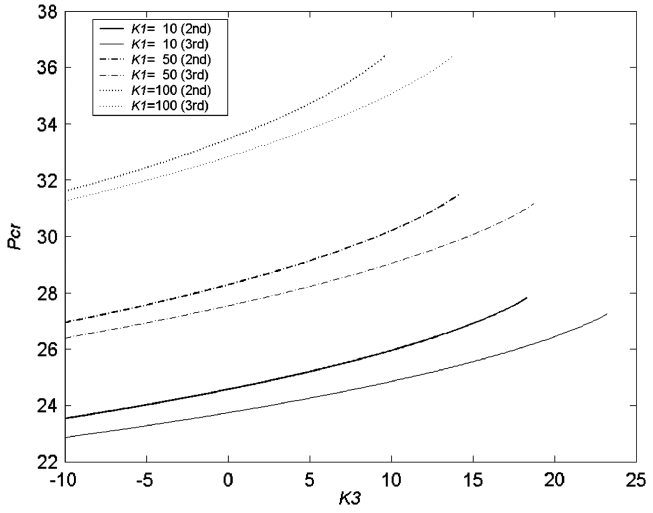

Fig. 3 Distribution of buckling load with foundation modulus ($\beta = 1$, $K_b = 2.0$, $K_i = 2.0$, $\nu = 0.3$, $H/h = 3$, $W_0 = 0$, $K_1 = 50$, $G = 0$).

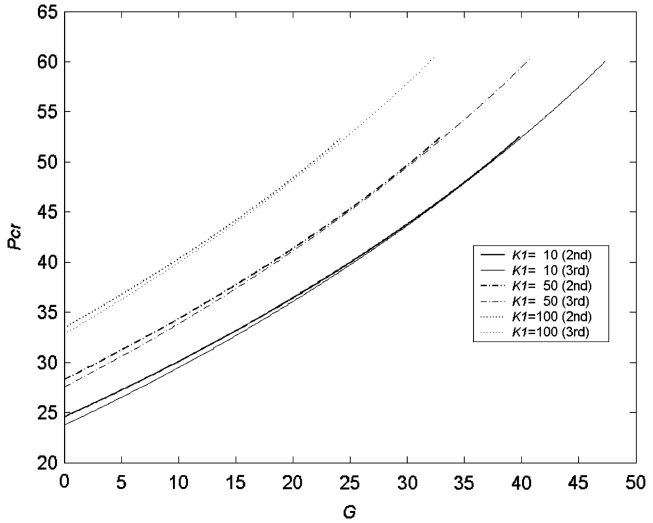

Fig. 4 Distribution of buckling load with foundation modulus ($\beta = 1$, $K_b = 2.0$, $K_i = 2.0$, $\nu = 0.3$, $H/h = 3$, $W_0 = 0$, $K_1 = 50$, $K_3 = 0$).

As the solution in Eq. (43) for the case of $p = \beta^{1/2} = 3$ is formulated independently in Sec III.C, continuity of the solution with Eq. (33) for $p \neq 3$ is also checked. Consider two cases of $p = 2.999$ and $p = 3.001$ using Eq. (33) and the case of $p = 3$ using Eq. (43), the corresponding expressions for the characteristic load-deflection relation for the case of $H/h = 3$, $K_b = 2.0$, $K_i = 2.0$, and $\nu = 0.3$ are given as

$$P = 18.7934W_m - 8.75052W_m^2 + 0.981814W_m^3 \quad \text{for } p = 2.999$$

$$P = 18.7895W_m - 8.74884W_m^2 + 0.981648W_m^3 \quad \text{for } p = 3.000$$

$$P = 18.7856W_m - 8.74716W_m^2 + 0.981481W_m^3 \quad \text{for } p = 3.001$$

It is clear that the values of the preceding three corresponding coefficients are almost the same, and the resulting solution for $p \neq 3$ in Eq. (33) can be used to replace the special solution of $p = 3$. The solution can thus be regarded as a unified solution for evaluating the mechanical behaviors of imperfect shells.

Furthermore, comparisons of the present results corresponding to the second approximation are made with available data based on the Garlerkin's method by Dumir [19] and presented in Figs. 5–7. It shows that the characteristic relation between external load and

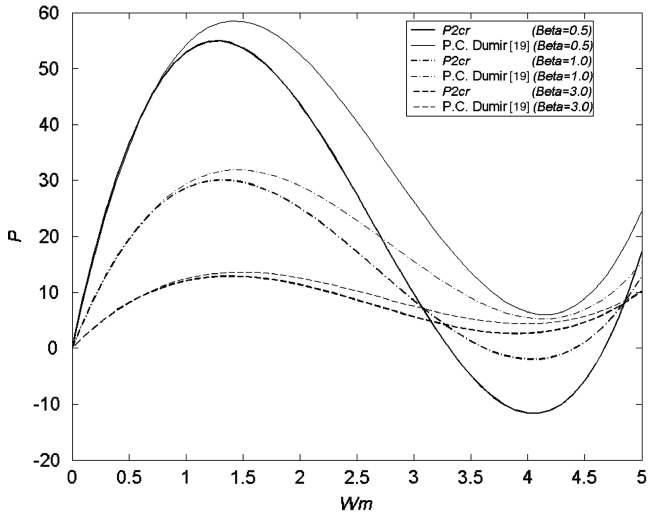

Fig. 5 Comparison of load deflection under different orthotropic parameters ($H/h = 3$, $K_b = K_i \to \infty$, $W_0 = 0$, $\nu = 0.3$, $K_1 = K_3 = G = 0$).

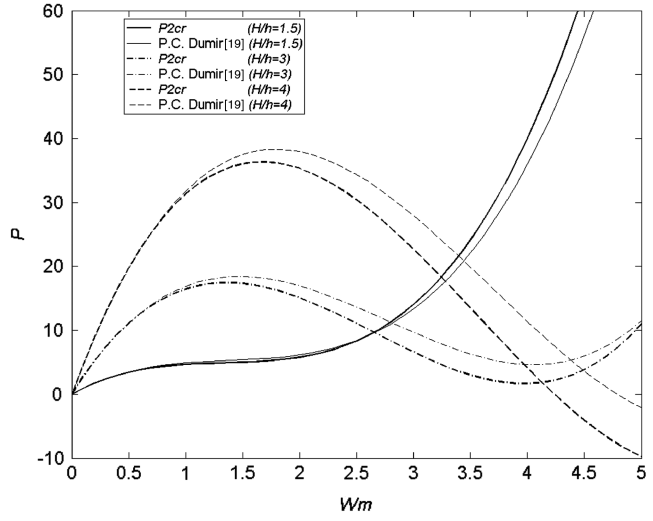

Fig. 6 Comparison of load deflection under different characteristic geometric parameters ($\beta = 2, K_b = K_i \to \infty, W_0 = 0, \nu = 0.3, K_1 = K_3 = G = 0$).

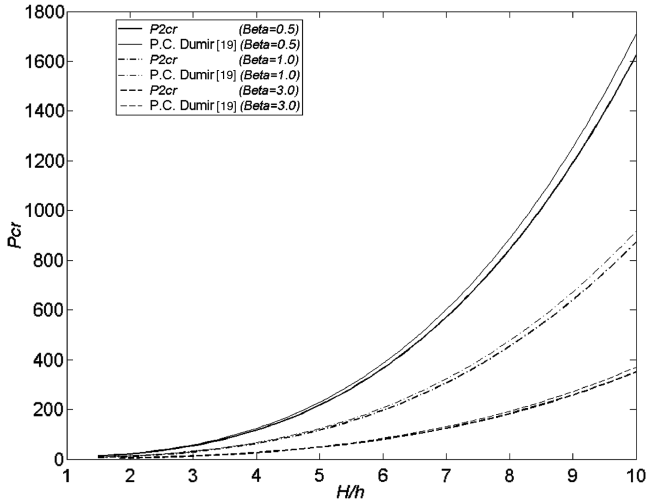

Fig. 7 Comparison of critical buckling load under different orthotropic parameters and characteristic geometric parameters ($K_b = K_i \to \infty$, $W_0 = 0$, $\nu = 0.3$, $K_1 = K_3 = G = 0$).

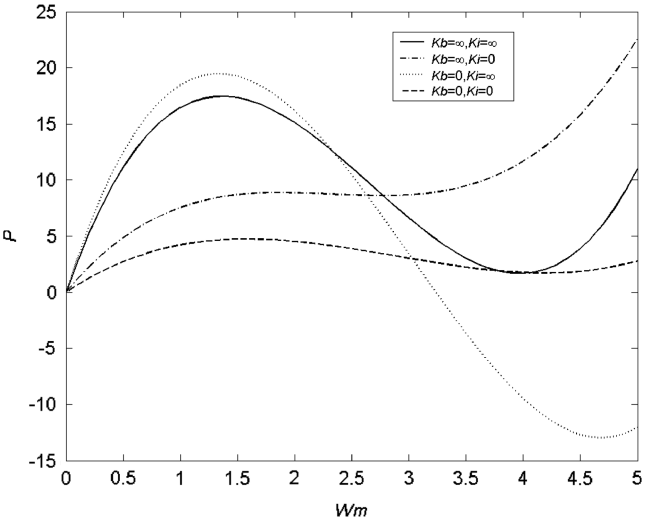

Fig. 9 Effect of classical boundary constraints on deformation of the shell ($\beta = 2$, $H/h = 3$, $W_0 = 0$, $\nu = 0.3$, $K_1 = K_3 = G = 0$).

central deflection for different orthotropic and geometric parameters of perfect shallow shells, with imperfection factor $W_0 = 0$, as shown in Figs. 5 and 6, agrees well with each other, especially for buckling loads.

For the case of normal pressure on the concave surface of an immovable, clamped perfect shell with geometrical and material parameters $\frac{H}{h} = 1.25$, $\beta = 1$, and $\nu = 0.3$, and moduli of foundation $K_1 = 20.0$, $K_3 = 0$, and $G = 10.0$, Fig. 8 compares the present results with known approximations based on Alpha method, Berger's method, modified Berger's method, and Sinharay and Banerjee's method as outlined by Paliwal and Bhalla [23]. It can be seen that solutions obtained by the present method are comparable to the more accurate modified Berger's method and Sinharay and Banerjee's method.

V. Effects of Parameters on Buckling of Orthotropic Shells

In the section, different factors on buckling behaviors are numerically investigated. First, consider the four classical boundary conditions formed by using special values of rotational and in-plane edge-restraint coefficients K_b and K_i such that 1) $K_b \to \infty$, $K_i \to \infty$; 2) $K_b \to \infty$, $K_i \to 0$; 3) $K_b \to 0$, $K_i \to \infty$; and 4) $K_b \to 0$, $K_i \to 0$, which correspond to immovable clamped, movable clamped, immovable simply supported, and movable simply supported edges, respectively. For a perfect orthotropic, shallow spherical shell with specific orthotropic parameter $\beta = 2$, ratio of apex height to thickness of the shell $H/h = 3$, and Poisson's ratio $\nu = \nu_\theta = 0.3$, the characteristic load-deflection relation is presented in Fig. 9. The snap-through buckling loads for immovable edge restraints are larger than for movable edge restraints. Also, the buckling load for movable clamped edge is larger than for movable simply supported edge. On the other hand, the buckling load for an immovable clamped edge is lower than for an immovable simply supported edge. These behaviors of the orthotropic, shallow spherical shell coincide with those in isotropic shells [7,27] and anisotropic reticulated shells [31].

Figure 10 shows the characteristic load-deflection relation for various ratios of apex height to thickness of the shell H/h. It can be seen that the snapping phenomenon occurs when the ratio exceeds a critical value. For the case of $\beta = 2$, $K_b = 2.0$, $K_i = 2.0$, and $\nu = 0.3$, the critical value of the ratio is approximately $H/h = 1.19$. For the case of the circular plate $H/h = 0$ the load increases monotonously with deflection. For the same boundary constraint condition, a change in the buckling load with characteristic geometric parameter is presented in Fig. 11. It indicates that a larger orthotropic parameter corresponds to a lower buckling load whereas a "deeper" shell has a higher buckling load. The effect of imperfection on the buckling load is shown in Fig. 12, which indicates that imperfection leads to a decrease in the buckling load.

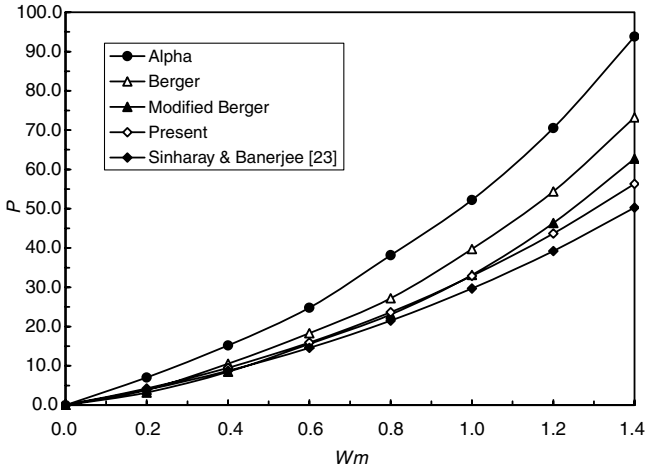

Fig. 8 Comparison of load-deflection relation using different methods ($H/h = 1.25$, $K_b = K_i \to \infty$, $W_0 = 0$, $\nu = 0.3$, $K_1 = 20.0$, $K_3 = 0.0$, $G = 10.0$).

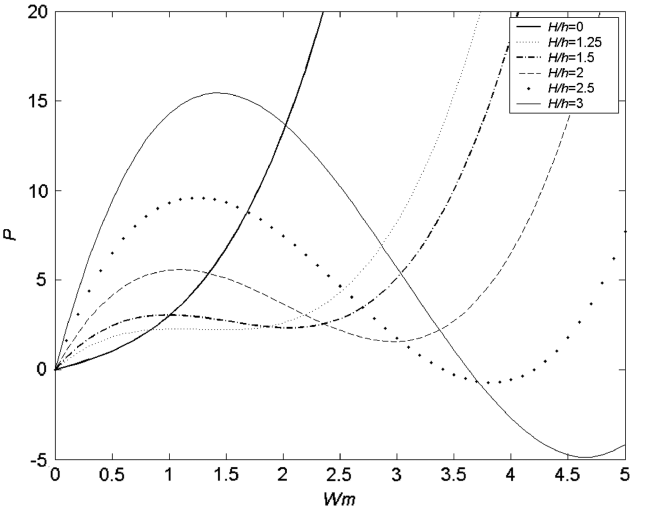

Fig. 10 Load deflection under different characteristic geometric parameters ($\beta = 2$, $K_b = 2.0$, $K_i = 2.0$, $\nu = 0.3$, $W_0 = 0$, $K_1 = K_3 = G = 0$).

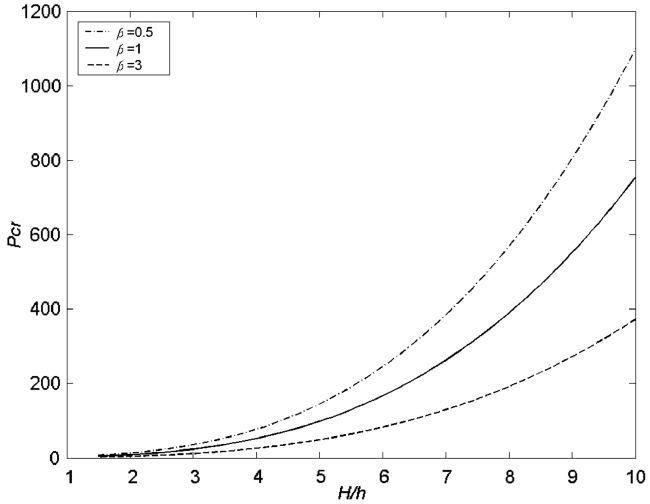

Fig. 11 Change in buckling load with characteristic geometrical parameters ($K_b = 2.0, K_i = 2.0, W_0 = 0, \nu = 0.3, K_1 = K_3 = G = 0$).

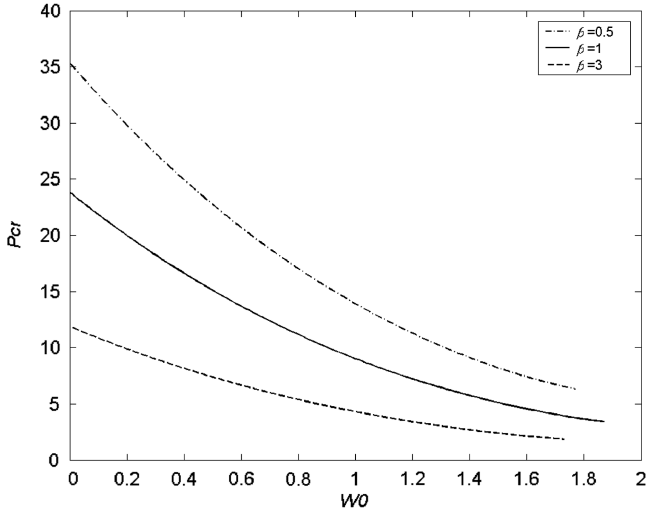

Fig. 12 Effect of imperfection on buckling load ($H/h = 3, K_b = 2.0, K_i = 2.0, \nu = 0.3, K_1 = K_3 = G = 0$).

For the case of the ratio of apex height to thickness of the shell $H/h = 3$ and rotational and in-plane edge-restraint coefficients $K_b = K_i = 2.0$, the effects of material parameters on buckling loads are presented in Figs. 13 and 14. As shown in Fig. 13, buckling load decreases considerably when there is an increase in the value of the orthotropic parameter β especially for $\beta < 1.0$. Figure 14 shows the relation between the buckling load and Possion's ratio ν, which indicates that when the orthotropic parameter $\beta < 1.0$, there will be a significant change in buckling load with an increase in Possion's ratio. However, when $\beta > 1.0$, the effect of Possion's ratio is very weak.

Figures 15 and 16 show the effects of rotational and in-plane edge-constraint coefficients K_b and K_i on buckling loads for different values of orthotropic parameter, respectively. When K_b or K_i are small ($K_b < 5.0$ or $K_i < 5.0$), buckling load increases with an increase in the edge-constraint coefficient. In particular, the buckling load increases significantly for small K_i. However, for higher values of K_b and K_i, a large increase in the two edge-constraint coefficients leads to a small change in buckling load. Specifically, the buckling load decreases gradually for increasing K_b, as shown in Fig. 15, although it increases slightly for increasing K_i, as shown in Fig. 16. Figure 16 also shows that the change of edge constraint from movable edge $K_i = 0.0$ to immovable edge with large K_i results in a large increase in the buckling load. Such a behavior is also shown in Fig. 9.

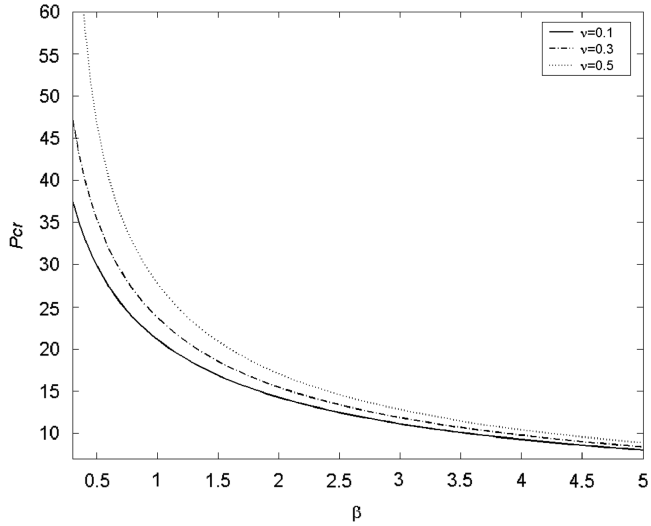

Fig. 13 Effect of orthotropic parameters on buckling load ($H/h = 3, K_b = 2.0, K_i = 2.0, W_0 = 0, \nu = 0.3, K_1 = K_3 = G = 0$).

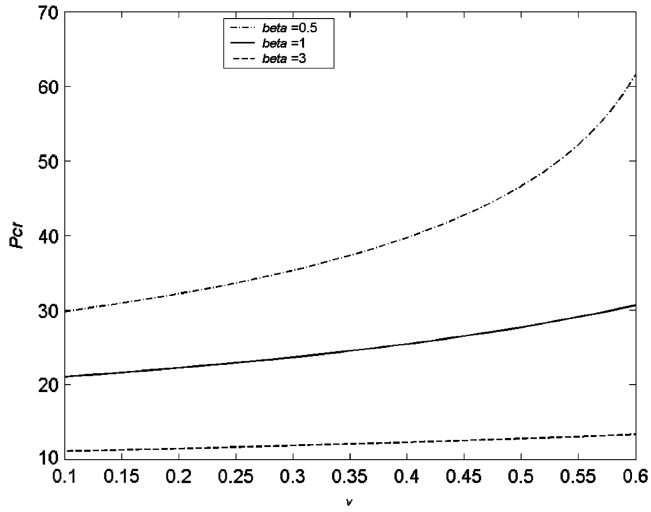

Fig. 14 Effect of Poisson's ratio on buckling load ($H/h = 3, K_b = 2.0, K_i = 2.0, W_0 = 0, K_1 = K_3 = G = 0$).

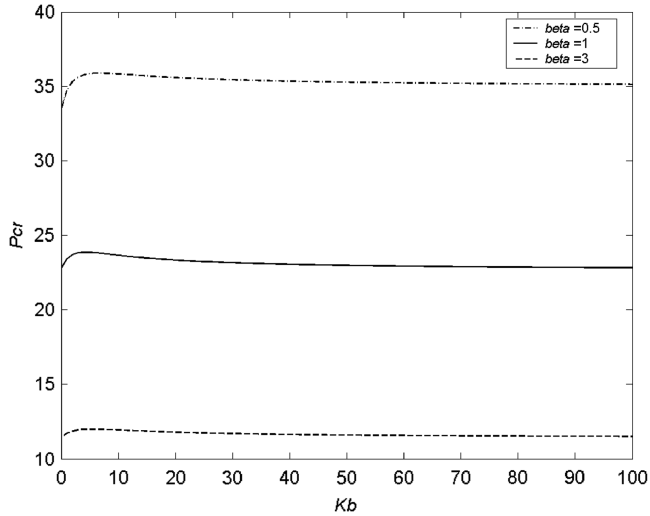

Fig. 15 Effect of rotational edge-constraint coefficient on buckling load ($H/h = 3, K_i = 2.0, W_0 = 0, \nu = 0.3, K_1 = K_3 = G = 0$).

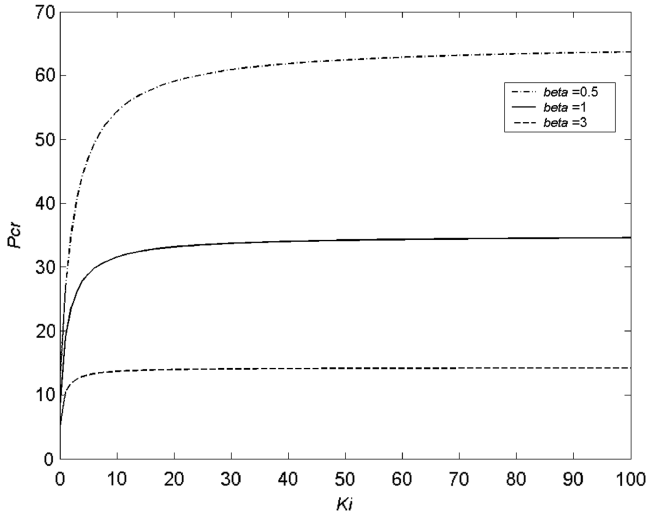

Fig. 16 Effect of in-plane edge-restraint coefficient on buckling load ($H/h = 3, K_b = 2.0, W_0 = 0, \nu = 0.3, K_1 = K_3 = G = 0$).

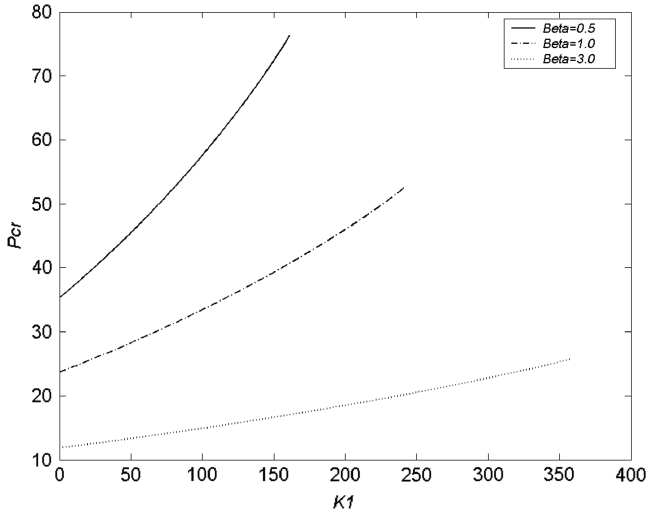

Fig. 17 Distribution of buckling load with the Young's modulus K_1 ($H/h = 3, K_b = 2.0, K_i = 2.0, W_0 = 0, \nu = 0.3, K_3 = G = 0$).

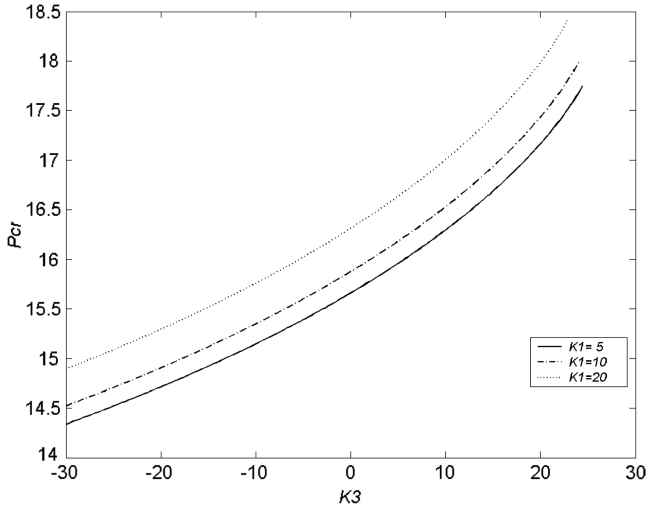

Fig. 18 Distribution of buckling load with the Young's modulus K_3 ($H/h = 3, K_b = 2.0, K_i = 2.0, W_0 = 0, \nu = 0.3, K_1 = 50, G = 0$).

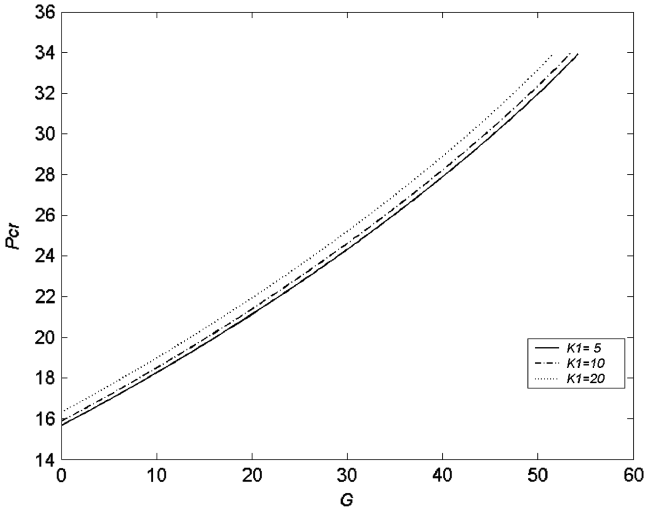

Fig. 19 Distribution of buckling load with shear modulus G ($H/h = 3, K_b = 2.0, K_i = 2.0, W_0 = 0, \nu = 0.3, K_1 = 50, K_3 = 0$).

Effects of Young's moduli K_1 and K_3 and shear modulus G of foundation on buckling loads of orthotropic shells are illustrated in Figs. 17–19. It can be seen that, in general, support of the elastic foundation on the shells results in high buckling loads. Figure 17 shows that the buckling load increases rapidly with an increase of the modulus K_1 for a smaller orthotropic parameter. Calculations predict that the modulus has its largest critical value, beyond which snapping phenomena no longer occurs. For a given geometry of the shell structure with an edge-constrain condition such as $H/h = 3$, $K_b = 2.0$, and $K_i = 2.0$, the critical values of the modulus are 161.95, 241.28, and 358.13 for the case of $\nu = 0.3$ and $\beta = 0.5$, 1.0, and 3.0, respectively. Similar behaviors appear for the effects of Young's modulus K_3 and shear modulus G. For the same geometry of the shell with three different orthotropic parameters $\beta = 0.5$, 1.0, and 3.0 with $\nu = 0.3$, the corresponding critical values of modulus K_3 are 24.56, 24.02, and 22.96, respectively, although the critical values of the modulus G are 54.39, 51.78, and 46.56, respectively, as can be seen from Figs. 18 and 19. From Fig. 18, it can also be seen that the two cases of $K_3 > 0$ and $K_3 < 0$ represent a hardening- and softening-type foundation, respectively. The buckling load tends to increase with a positive modulus and decreases with a negative modulus.

VI. Conclusions

This paper presents an asymptotic solution for nonlinear buckling of elastically restrained imperfect orthotropic, shallow spherical shells on an elastic foundation. The analytic and explicit characteristic load-deflection relation is formulated in nondimensional form. The solution incorporates effects of various factors, including orthotropic and material parameters, geometric imperfection factor, Young's and shear moduli of foundation, and edge-restraint coefficients. The method can be used to evaluate nonlinear deformation and buckling behaviors of orthotropic imperfect shallow spherical shells. A parametric analysis is carried out in detail for deformation and buckling of such structures. Comparisons with available data for several specific cases show that the resulting solution is accurate in terms of computation.

Appendix A: Expressions for Coefficients b_{ij} and c_{si} for $p \neq 3$

$$b_{11} = -\frac{eW_0(1+p)a_1^2}{1+3p}, \qquad b_{12} = -\frac{1}{4}e\lambda a_1$$

$$b_{13} = -\frac{eW_0(1+p)a_1a_2}{2+p}$$

$$b_{14}=-\frac{4e\lambda a_2}{25-p^2},\qquad b_{15}=\frac{16eW_0a_2^2}{49-p^2},\qquad b_{21}=-\frac{e(1+p)a_1^2}{2(1+3p)}$$
$$b_{22}=-\frac{e(1+p)a_1a_2}{2(2+p)},\qquad b_{23}=\frac{8ea_2^2}{49-p^2}$$

$$c_{31}=\frac{a_1b_{20}}{2(1+p)(1+3p)},\qquad c_{32}=-\frac{K_3}{8(9-p^2)}$$
$$c_{33}=\frac{a_1b_{21}}{12(1+p)(1+2p)}$$

$$b_{10}=\frac{(1+2p-B_i)b_{11}+(2+p-B_i)b_{12}+(4+p-B_i)b_{13}+(5-B_i)b_{14}+(7-B_i)b_{15}}{B_i-p}$$

$$b_{20}=\frac{(1+2p-B_i)b_{21}+(4+p-B_i)b_{22}+(7-B_i)b_{23}}{B_i-p}$$

$$c_{11}=\frac{a_1b_{10}W_0}{2(1+p)(1+3p)},\qquad c_{12}=\frac{\lambda b_{10}+G(1+p)a_1}{4(1+p)(3+p)}$$
$$c_{13}=-\frac{K_1}{8(9-p^2)}$$

$$c_{14}=\frac{a_1b_{10}W_0}{12(1+p)(1+2p)},\qquad c_{15}=\frac{\lambda b_{11}+(1+p)a_1b_{12}W_0}{6(1+p)(2+p)(3+p)}$$
$$c_{16}=-\frac{K_1a_1}{8(2+p)(3+p)(5+p)}$$

$$c_{17}=\frac{2Ga_2}{3(25-p^2)},\qquad c_{18}=\frac{[(1+p)a_1b_{13}+4a_2b_{11}]W_0}{2(3+p)(5+p)(5+3p)}$$
$$c_{19}=\frac{\lambda b_{13}+(1+p)W_0a_1b_{14}+4W_0a_2b_{12}}{12(3+p)(7+p)}$$

$$c_{110}=\frac{6\lambda b_{14}-K_1a_2}{48(49-p^2)},\qquad c_{111}=\frac{[(1+p)a_1b_{15}+4a_2b_{13}]W_0}{16(4+p)(9+p)}$$

$$c_{112}=\frac{\lambda b_{15}+4W_0a_2b_{14}}{10(81-p^2)},\qquad c_{113}=\frac{a_2b_{15}W_0}{3(121-p^2)}$$

$$c_{21}=\frac{a_1(b_{10}+b_{20}W_0)}{2(1+p)(1+3p)},\qquad c_{22}=\frac{\lambda b_{20}}{4(1+p)(3+p)}$$
$$c_{23}=\frac{a_1(b_{11}+W_0b_{21})}{12(1+p)(1+2p)}$$

$$c_{24}=\frac{\lambda b_{21}+(1+p)a_1b_{12}}{6(1+p)(2+p)(3+p)},\quad c_{25}=\frac{\lambda b_{12}+4a_2(W_0b_{10}+b_{20})}{8(2+p)(5+p)}$$

$$c_{26}=\frac{4a_2(b_{11}+W_0b_{21})+(1+p)a_1(b_{13}+W_0b_{22})}{2(3+p)(5+p)(5+3p)}$$
$$c_{27}=\frac{\lambda b_{22}+(1+p)a_1b_{14}+4a_2b_{12}}{12(3+p)(7+p)}$$

$$c_{28}=\frac{\lambda b_{14}}{8(49-p^2)}$$
$$c_{29}=\frac{4a_2(b_{13}+W_0b_{22})+(1+p)a_1(b_{15}+W_0b_{23})}{16(4+p)(9+p)}$$

$$c_{210}=\frac{\lambda b_{23}+4a_2b_{14}}{10(81-p^2)},\qquad c_{211}=\frac{a_2(b_{15}+W_0b_{23})}{3(121-p^2)}$$

$$c_{34}=-\frac{3K_3a_1}{8(2+p)(3+p)(5+p)}$$

$$c_{35}=\frac{2(1+p)(2+p)a_1b_{22}+8(1+p)a_2b_{21}-3K_3a_1^2}{4(2+p)(3+p)(5+p)(5+3p)}$$

$$c_{36}=-\frac{K_1a_2}{16(49-p^2)}$$

$$c_{37}=-\frac{K_1a_1^3}{4(3+p)(3+2p)(5+3p)(7+3p)}$$

$$c_{38}=\frac{(1+p)(7+p)a_1b_{23}+4(7+p)a_2b_{22}-6K_3a_1a_2}{16(4+p)(7+p)(9+p)}$$

$$c_{39}=\frac{-K_3a_1^2a_2}{4(3+p)(4+p)(5+p)(9+p)}$$

$$c_{310}=\frac{a_2(40b_{23}-K_3a_2)}{120(121-p^2)}$$
$$c_{311}=\frac{-K_3a_1a_2^2}{8(6+p)(11+p)(13+p)}$$

$$c_{312}=\frac{-K_3a_2^3}{224(225-p^2)}$$

$$\begin{aligned}c_{10}=\Bigg[&-4(B_b+3)\left(1+\sum_{i=1}^{13}c_{1i}\right)+2(1+p)(1+2p+B_b)c_{11}\\&+(2+p+B_b)(3+p)c_{12}+4(3+B_b)c_{13}\\&+3(1+p)(2+3p+B_b)c_{14}+2(2+p)(3+2p+B_b)c_{15}\\&+(5+p)(4+p+B_b)c_{16}+6(5+B_b)c_{17}\\&+2(3+p)(5+2p+B_b)c_{18}+(7+p)(6+p+B_b)c_{19}\\&+8(7+B_b)c_{110}+(9+p)(8+p+B_b)c_{111}\\&+10(9+B_b)c_{112}+12(11+B_b)c_{113}\Bigg]\Big/\Big[4(B_b+3)\\&-(p+B_b)(1+p)\Big]\end{aligned}$$

$$\begin{aligned}c_{20}=\Bigg[&-4(B_b+3)\sum_{i=1}^{11}c_{2i}+2(1+p)(1+2p+B_b)c_{21}\\&+(2+p+B_b)(3+p)c_{22}+3(1+p)(2+3p+B_b)c_{23}\\&+2(2+p)(3+2p+B_b)c_{24}+(5+p)(4+p+B_b)c_{25}\\&+2(3+p)(5+2p+B_b)c_{26}+(7+p)(6+p+B_b)c_{27}\\&+8(7+B_b)c_{28}+(9+p)(8+p+B_b)c_{29}\\&+10(9+B_b)c_{210}+12(11+B_b)c_{211}\Bigg]\Big/\Big[4(B_b+3)\\&-(p+B_b)(1+p)\Big]\end{aligned}$$

$$c_{30} = \Big[-4(B_b+3)\sum_{i=1}^{12} c_{3i} + 2(1+p)(1+2p+B_b)c_{31} + 4(3+B_b)c_{32} + 3(1+p)(2+3p+B_b)c_{33} + (5+p)(4+p+B_b)c_{34} + 2(3+p)(5+2p+B_b)c_{35} + 8(7+B_b)c_{36} + (7+3p)(6+3p+B_b)c_{37} + (9+p)(8+p+B_b)c_{38} + 2(5+p)(9+2p+B_b)c_{39} + 12(11+B_b)c_{310} + (13+p)(12+p+B_b)c_{311} + 16(15+B_b)c_{312}\Big] \Big/ \Big[4(B_b+3) - (p+B_b)(1+p)\Big]$$

Appendix B: Expressions for Coefficients b_{ij} and c_{si} for $p = 3$

$$b_{11} = -\frac{1}{32}e\lambda(8a_4 - 5a_5), \qquad b_{12} = -\frac{1}{4}e\lambda a_5$$

$$b_{13} = -\frac{1}{500}eW_0(200a_4^2 - 140a_4a_5 + 39a_5^2)$$

$$b_{14} = -\frac{1}{25}eW_0(20a_4 - 7a_5)a_5, \qquad b_{15} = -\frac{2}{5}eW_0a_5^2$$

$$b_{21} = -\frac{1}{1000}e(200a_4^2 - 140a_4a_5 + 39a_5^2)$$

$$b_{22} = -\frac{1}{50}e(20a_4 - 7a_5)a_5, \qquad b_{23} = -\frac{1}{5}ea_5^2$$

$$b_{10} = \frac{(1+2p-B_i)b_{11} + (2+p-B_i)b_{12} + (4+p-B_i)b_{13} + (5-B_i)b_{14} + (7-B_i)b_{15}}{B_i - p}$$

$$b_{20} = \frac{(1+2p-B_i)b_{21} + (4+p-B_i)b_{22} + (7-B_i)b_{23}}{B_i - p}$$

$$c_{11} = \frac{K_1}{72}, \qquad c_{12} = \frac{K_1}{12}, \qquad c_{13} = \frac{1}{32}[G(8a_4 - 5a_5) + 2\lambda b_{10}]$$

$$c_{14} = \frac{Ga_5}{4}$$

$$c_{15} = \frac{W_0(20a_4 - 7a_5)b_{10}}{200} + \frac{\lambda(20b_{11} - 7b_{12})}{800} - \frac{K_1(30a_4 - 23a_5)}{7200}$$

$$c_{16} = \frac{1}{10}W_0a_5b_{10} + \frac{1}{40}\lambda b_{12} - \frac{1}{240}K_1a_5$$

$$c_{17} = \frac{W_0[18a_4(4b_{11} - b_{12}) - a_5(18b_{11} - 7b_{12})]}{1296} + \frac{\lambda(72b_{13} - 18b_{14} + 7b_{15})}{5184}$$

$$c_{18} = \frac{W_0[2a_4b_{12} - a_5(2b_{11} - b_{12})]}{36} + \frac{\lambda(2b_{14} - b_{15})}{144}$$

$$c_{19} = \frac{1}{18}W_0a_5b_{12} + \frac{1}{72}\lambda b_{15}$$

$$c_{110} = W_0\Big[a_4\Big(\frac{1}{28}b_{13} - \frac{11}{1568}b_{14} + \frac{93}{43904}b_{15}\Big) - a_5\Big(\frac{11}{1568}b_{13} - \frac{93}{43904}b_{14} + \frac{2145}{2458624}b_{15}\Big)\Big]$$

$$c_{111} = \frac{1}{28}W_0a_5b_{15}, \qquad c_{21} = \frac{1}{16}\lambda b_{20}$$

$$c_{22} = \frac{(20a_4 - 7a_5)(b_{10} + W_0b_{20})}{200}$$

$$c_{23} = \frac{1}{10}(a_4b_{10} + W_0a_5b_{20})$$

$$c_{24} = \frac{18a_4(4b_{11} - b_{12}) - a_5(18b_{11} - 7b_{12})}{1296} + \frac{\lambda(72b_{21} - 18b_{22} + 7b_{23})}{5184}$$

$$c_{25} = \frac{2a_4b_{12} + a_5(2b_{11} - b_{12})}{36} + \frac{\lambda(2b_{22} - b_{23})}{144}$$

$$c_{26} = \frac{1}{18}a_5b_{12} + \frac{1}{72}\lambda b_{23}$$

$$c_{27} = a_4\Big(\frac{1}{28}b_{13} - \frac{11}{1568}b_{14} + \frac{93}{43904}b_{15}\Big) - a_5\Big(\frac{11}{1568}b_{13} - \frac{93}{43904}b_{14} + \frac{2145}{2458624}b_{15}\Big) + W_0\Big[a_4\Big(\frac{1}{28}b_{21} - \frac{11}{1568}b_{22} + \frac{93}{43904}b_{23}\Big) - a_5\Big(\frac{11}{1568}b_{21} - \frac{93}{43904}b_{22} + \frac{2145}{2458624}b_{23}\Big)\Big]$$

$$c_{28} = a_4\Big(\frac{1}{28}b_{14} - \frac{11}{784}b_{15}\Big) + a_5\Big(\frac{1}{28}b_{13} - \frac{11}{784}b_{14} + \frac{279}{43904}b_{15}\Big) + W_0\Big[a_4\Big(\frac{1}{28}b_{22} - \frac{11}{784}b_{23}\Big) + a_5\Big(\frac{1}{28}b_{21} - \frac{11}{784}b_{22} + \frac{279}{43904}b_{23}\Big)\Big]$$

$$c_{29} = \frac{1}{28}a_4b_{15} + a_5\Big(\frac{1}{28}b_{14} - \frac{33}{1568}b_{15}\Big) + W_0\Big[\frac{1}{28}a_4b_{23} + a_5\Big(\frac{1}{28}b_{22} - \frac{33}{1568}b_{23}\Big)\Big]$$

$$c_{210} = \frac{1}{28}a_5(b_{15} + W_0b_{23}), \qquad c_{31} = \frac{K_3}{72}$$

$$c_{32} = -\frac{K_3}{12}$$

$$c_{33} = \frac{(20a_4 - 7a_5)b_{20}}{200} - \frac{(30a_4 - 23a_5)K_3}{2400}$$
$$c_{34} = \frac{a_5(8b_{20} - K_3)}{80}$$

$$c_{35} = a_4\left(\frac{1}{28}b_{21} - \frac{11}{1568}b_{22} + \frac{93}{43904}b_{23}\right) - a_5\left(\frac{11}{1568}b_{21} - \frac{93}{43904}b_{22} + \frac{2145}{2458624}b_{23}\right) - K_3\left(\frac{3}{1120}a_4^2 - \frac{459}{156800}a_4a_5 + \frac{38727}{43904000}a_5^2\right)$$

$$c_{36} = a_4\left(\frac{1}{28}b_{22} - \frac{11}{784}b_{23}\right) + a_5\left(\frac{1}{28}b_{21} - \frac{11}{784}b_{22} + \frac{279}{43904}b_{23}\right) - K_3a_5\left(\frac{3}{560}a_4 - \frac{459}{156800}a_5\right)$$

$$c_{37} = \frac{1}{28}a_4b_{23} + a_5\left(\frac{1}{28}b_{22} - \frac{33}{1568}b_{23}\right) - \frac{3}{1120}K_3a_5^2, \qquad c_{38} = \frac{1}{28}a_5b_{23}$$

$$c_{39} = K_3\left(-\frac{1}{3024}a_4^3 + \frac{29}{63504}a_4^2a_5 - \frac{14417}{64012032}a_4a_5^2 + \frac{321833}{8065516032}a_5^3\right)$$

$$c_{310} = K_3a_5\left(-\frac{1}{1008}a_4^2 + \frac{29}{31572}a_4a_5 - \frac{14417}{64012032}a_5^2\right)$$

$$c_{311} = K_3a_5\left(-\frac{1}{1008}a_4 + \frac{29}{63504}a_5\right), \qquad c_{312} = -\frac{1}{3024}K_3a_5^3$$

$$c_{10} = -\frac{1}{4(B_b+7)}\left[7c_{11} + \frac{23c_{13}}{3} + \frac{5c_{14}}{9} + 9c_{15} + \frac{3c_{16}}{4} + \frac{53c_{17}}{5} + \frac{21c_{18}}{25} + \frac{4c_{19}}{125} + \frac{37c_{110}}{3} + \frac{8c_{111}}{9} + \frac{c_{112}}{54} - \frac{c_{113}}{216} + B_b(c_{11} + c_{13} + c_{15} + c_{17} + c_{110})\right]$$

$$c_{20} = -\frac{1}{4(B_b+7)}\left[\frac{23c_{21}}{3} + 9c_{22} + \frac{3c_{23}}{4} + \frac{53c_{24}}{5} + \frac{21c_{25}}{25} + \frac{4c_{26}}{125} + \frac{37c_{27}}{3} + \frac{8c_{28}}{9} + \frac{c_{29}}{54} - \frac{c_{210}}{216} + B_b(c_{21} + c_{22} + c_{24} + c_{27})\right]$$

$$c_{30} = -\frac{1}{4(B_b+7)}\left[7c_{31} + 9c_{33} + \frac{3c_{34}}{4} + \frac{37c_{35}}{3} + \frac{8c_{36}}{9} + \frac{c_{37}}{54} - \frac{c_{38}}{216} + 16c_{39} + \frac{15c_{310}}{16} + \frac{c_{311}}{128} - \frac{c_{312}}{2048} + B_b(c_{31} + c_{33} + c_{35} + c_{39})\right]$$

Acknowledgments

This work is partially supported by the research committee of the Hong Kong Polytechnic University (Grant No. G-YF70). Support from the Program for New Century Excellent Talents in Universities by the Ministry of Education of China (Grant No. NCET-04-0373) and the Program for Shanghai Key Discipline of Solid Mechanics are also greatly acknowledged. The authors also wish to acknowledge the valuable comments of the reviewers for improving the presentation of the paper.

References

[1] Archer, R. R., "Stability Limits for a Clamped Spherical Shell Segment Under Uniform Pressure," *Quarterly of Applied Mathematics*, Vol. 15, No. 4, 1957, pp. 355–366.

[2] Thurston, G. A., "A Numerical Solution of the Nonlinear Equations for Axisymmetric Bending of Shallow Spherical Shells," *Journal of Applied Mechanics*, Vol. 28, No. 4, 1961, pp. 557–562.

[3] Huang, N., "Unsymmetrical Buckling of Thin Shallow Spherical Shells," *Journal of Applied Mechanics*, Vol. 31, No. 3, 1964, pp. 447–457.

[4] Famili, J., and Archer, R. R., "Finite Asymmetric Deformation of Shallow Spherical Shells," *AIAA Journal*, Vol. 3, No. 3, 1964, pp. 506–510.

[5] Stephens, W. B., and Fulton, R. E., "Axisymmetric Static and Dynamic Buckling of Spherical Caps due to Centrally Distributed Pressure," *AIAA Journal*, Vol. 7, No. 11, 1969, pp. 2120–2126. doi:10.2514/3.5567

[6] Varadan, T. K., "Snap-Buckling of Orthotropic Shallow Spherical Shells," *Journal of Applied Mechanics*, Vol. 45, No. 2, 1978, pp. 445–447.

[7] Dumir, P. C., Gandhi, M. L., and Nath, Y., "Axisymmetric Static and Dynamic Buckling of Orthotropic Shallow Spherical Caps with Flexible Supports," *Acta Mechanica*, Vol. 52, Nos. 1–2, 1984, pp. 93–106. doi:10.1007/BF01175967

[8] Yamada, S., and Yamada, M., "Buckling and Postbuckling Behavior of Half-Loaded Shallow Spherical Shells," *International Journal of Non-Linear Mechanics*, Vol. 20, No. 4, 1985, pp. 239–248. doi:10.1016/0020-7462(85)90032-0

[9] Brodland, G. W., and Cohen, H., "Deflection and Snapping of Spherical Caps," *International Journal of Solids and Structures*, Vol. 23, No. 10, 1987, pp. 1341–1356. doi:10.1016/0020-7683(87)90001-1

[10] Grigolyuk, E. I., and Lopanitsyn, Y. A., "The Non-Axisymmetric Postbuckling Behavior of Shallow Spherical Domes," *Journal of Applied Mechanics*, Vol. 67, No. 6, 2003, pp. 809–818. doi:10.1016/S0021-8928(03)90501-6

[11] Li, Q. S., Liu, J., and Tang, J., "Buckling of Shallow Spherical Shells Including the Effects of Transverse Shear Deformation," *International Journal of Mechanical Sciences*, Vol. 45, No. 9, 2003, pp. 1519–1529. doi:10.1016/j.ijmecsci.2003.09.020

[12] Btachut, J., "Buckling of Shallow Spherical Caps Subjected to External Pressure," *Journal of Applied Mechanics*, Vol. 72, No. 5, 2005, pp. 803–806. doi:10.1115/1.1993667

[13] Hutchinson, J. W., "Imperfection Sensitivity of Externally Pressurized Spherical Shells," *Journal of Applied Mechanics*, Vol. 34, No. 1, 1967, pp. 49–55.

[14] Koga, T., and Hoff, N. J., "The Axisymmetric Buckling of Initial Imperfection Complete Spherical Shells," *International Journal of Solids and Structures*, Vol. 5, No. 7, 1969, pp. 679–697. doi:10.1016/0020-7683(69)90088-2

[15] Kao, R., "A Note on Buckling of Spherical Caps with Initial Asymmetric Imperfections," *Journal of Applied Mechanics*, Vol. 39, No. 3, 1972, pp. 842–844.

[16] Ory, H., Reimerdes, H. G., Schmid, T., Rittweger, A., and Gomez Garcia, J., "Imperfection Sensitivity of an Orthotropic Spherical Shell Under External Pressure," *International Journal of Non-Linear Mechanics*, Vol. 37, Nos. 4–5, 2002, pp. 669–686. doi:10.1016/S0020-7462(01)00091-9

[17] Wunderlich, W., and Albertin, U., "Buckling Behaviour of Imperfect Spherical Shells," *International Journal of Non-Linear Mechanics*, Vol. 37, Nos. 4–5, 2002, pp. 589–604. doi:10.1016/S0020-7462(01)00086-5

[18] Nath, Y., and Jain, R. K., "Non-Linear Dynamic Analysis of Shallow Spherical Shells on Elastic Foundations," *International Journal of Mechanical Sciences*, Vol. 25, No. 6, 1983, pp. 409–419. doi:10.1016/0020-7403(83)90055-3

[19] Dumir, P. C., "Nonlinear Axisymmetric Response of Orthotropic Thin Spherical Caps on Elastic Foundations," *International Journal of*

Mechanical Sciences, Vol. 27, No. 11–12, 1985, pp. 751–760. doi:10.1016/0020-7403(85)90007-4

[20] Jain, R. K., and Nath, Y., "Effect of Foundation Nonlinearity on Nonlinear Transient Response of Orthotropic Shallow Spherical Shells," *Ingenieur-Archiv*, Vol. 56, No. 4, 1986, pp. 295–300. doi:10.1007/BF00542480

[21] Paliwal, D. N., Sinha, S. N., and Choudhary, B. K., Jr., "Shallow Spherical Shells on Pasternak Foundation," *Journal of Engineering Mechanics*, Vol. 112, No. 2, 1986, pp. 175–182. doi:10.1061/(ASCE)0733-9399(1986)112:2(175)

[22] Paliwal, D. N., and Sinha, S. N., "Static and Dynamic Behavior of Shallow Spherical Shells on Winkler Foundation," *Thin-Walled Structures*, Vol. 4, No. 6, 1986, pp. 411–422. doi:10.1016/0263-8231(86)90038-8

[23] Paliwal, D. N., and Bhalla, V., "Large Deflection Analysis of a Shallow Spherical Shell on Pasternak Foundation," *International Journal of Pressure Vessels and Piping*, Vol. 52, No. 2, 1992, pp. 189–199. doi:10.1016/0308-0161(92)90015-8

[24] Paliwal, D. N., and Srivastava, R., "Nonlinear Static Behaviour of Shallow Spherical Shell on a Kerr Foundation," *International Journal of Pressure Vessels and Piping*, Vol. 55, No. 3, 1993, pp. 481–494. doi:10.1016/0308-0161(93)90065-2

[25] Kanagasabapathy, H., Paliwal, D. N., and Gupta, K. M., "Large Deflection of an Orthotropic Shallow Spherical Shell on a Pasternak Foundation," *International Journal of Pressure Vessels and Piping*, Vol. 62, No. 2, 1995, pp. 117–122. doi:10.1016/0308-0161(95)93968-B

[26] Paliwal, D. N., Kanagasabapathy, H., and Gupta, K. M., "Orthotropic Shallow Spherical Shell on a Kerr Foundation," *Journal of Pressure Vessel Technology*, Vol. 119, No. 1, 1997, pp. 131–133. doi:10.1115/1.2842258

[27] Nie, G. H., "Asymptotic Buckling Analysis of Imperfect Shallow Spherical Shells on Non-Linear Elastic Foundation," *International Journal of Mechanical Sciences*, Vol. 43, No. 2, 2001, pp. 543–555. doi:10.1016/S0020-7403(99)00118-6

[28] Nie, G. H., "Analysis of Non-Linear Behaviors of Imperfect Shallow Spherical Shells on Pasternak Foundation by the Asymptotic Iteration Method," *International Journal of Pressure Vessels and Piping*, Vol. 80, No. 4, 2003, pp. 229–235. doi:10.1016/S0308-0161(03)00043-7

[29] Nie, G. H., and Cheung, Y. K., "A Non-Linear Model for Stability Analysis of Reticulated Shallow Shells with Imperfections," *International Journal of Space Structures*, Vol. 10, No. 4, 1995, pp. 215–230.

[30] Nie, G. H., "Non-Linear Free Vibration of Single-Layer Reticulated Shallow Spherical Shells," *International Journal of Space Structures*, Vol. 15, No. 1, 2000, pp. 53–58.

[31] Nie, G. H., "On the Buckling of Imperfect Squarely-Reticulated Shallow Spherical Shells Supported by Elastic Media," *Thin-Walled Structures*, Vol. 41, No. 1, 2003, pp. 1–13. doi:10.1016/S0263-8231(02)00069-1

A. Palazotto
Associate Editor